Eur. Phys. J. B **48**, 167–171 (2005)
DOI: 10.1140/epjb/e2005-00400-4

THE EUROPEAN PHYSICAL JOURNAL B

A simple method for the determination of strains in epitaxial films: application to Eu(110) deposited on a Nb(110) buffer

S. Soriano[1], T. Gourieux[1], A. Stunault[2], K. Dumesnil[1], and C. Dufour[1,a]

[1] Laboratoire de Physique des Matériaux, UMR CNRS 7556, Université Henri Poincaré, BP 239, 54506 Vandoeuvre-lès-Nancy, France
[2] Institut Laue-Langevin, 6 rue Jules Horowitz, BP 156, 38042 Grenoble Cedex 9, France

Received 19 July 2005
Published online 16 December 2005 –

Abstract. In order to determine the strain tensor in a 375 nm thick Eu(110) epitaxial thin film, we have developed a new method, based on the accurate determination of the lattice vectors by high resolution X-ray diffraction. We show that a biaxial strain model gives a good representation of the state of the strains field in the film.

PACS. 75.70.-i Magnetic properties of thin films, surfaces, and interfaces – 61.10.Nz X-ray diffraction – 68.55.-a Thin films structure and morphology

Introduction

Strains in a material may greatly influence its physical properties. In particular, in magnetic epitaxial thin films, the strains, arising from either epitaxial stresses or clamping effects with the substrate, can modify the magnetoelastic energy terms so that the resulting magnetic properties differ from the bulk ones [1]. Strains and stresses determination is usually achieved by X-ray diffraction using the so-called "$\sin^2\psi$" method, well suited for the case of polycrystalline or textured thin films [2]. When the film is, in a first approximation, a thin single crystal, one can actually use a more direct method, based on the accurate determination of the lattice vectors of the strained film from the measured positions of Bragg peaks in 3-dimensional reciprocal space. In the following we develop this simple method for the determination of the strain tensor in a cubic single crystal and apply it to the study of the temperature dependent strains in a Eu(110) epitaxial thin film. This work is part of a study of epitaxial Eu thin films, for which the magnetic behaviour differs from that of bulk Eu, and depends on the film thickness [3].

Strain determination

The method is presented in an intuitive way in the framework of the cubic symmetry of bcc Eu. The generalisation to more complex cases is straightforward.

We assume that we can define a homogeneous (average) strain field inside the film, or at least inside the X-ray probed sample region. The epitaxial thin film is described as a single crystal with unknown lattice vectors $(\boldsymbol{a}, \boldsymbol{b}, \boldsymbol{c})$ deviating from the known conventional cubic lattice vectors $(\boldsymbol{a}_0, \boldsymbol{b}_0, \boldsymbol{c}_0)$ of an hypothetical unstrained sample by small vectors deviations $(\boldsymbol{\delta a}, \boldsymbol{\delta b}, \boldsymbol{\delta c})$ in such a way that:

$$\begin{cases} \boldsymbol{a} = \boldsymbol{a}_0 + \boldsymbol{\delta a} \\ \boldsymbol{b} = \boldsymbol{b}_0 + \boldsymbol{\delta b} \\ \boldsymbol{c} = \boldsymbol{c}_0 + \boldsymbol{\delta c}. \end{cases} \tag{1}$$

We can express $(\boldsymbol{\delta a}, \boldsymbol{\delta b}, \boldsymbol{\delta c})$ in the orthonormal basis $(\boldsymbol{u}_x, \boldsymbol{u}_y, \boldsymbol{u}_z)$where $\boldsymbol{u}_x$, $\boldsymbol{u}_y$ and $\boldsymbol{u}_z$ are unit vectors along $\boldsymbol{a}_0$, $\boldsymbol{b}_0$ and $\boldsymbol{c}_0$ respectively:

$$\begin{cases} \boldsymbol{\delta a} = \delta a_x\ \boldsymbol{u}_x + \delta a_y\ \boldsymbol{u}_y + \delta a_z\ \boldsymbol{u}_z \\ \boldsymbol{\delta b} = \delta b_x\ \boldsymbol{u}_x + \delta b_y\ \boldsymbol{u}_y + \delta b_z\ \boldsymbol{u}_z \\ \boldsymbol{\delta c} = \delta c_x\ \boldsymbol{u}_x + \delta c_y\ \boldsymbol{u}_y + \delta c_z\ \boldsymbol{u}_z. \end{cases} \tag{2}$$

Actually, it is easy to show that the nine components of the lattice vectors deviations identify to the components of the so-called distortion tensor $\overleftrightarrow{\gamma}$ except for a a_0 factor corresponding to the (unstrained) cubic lattice constant:

$$\overleftrightarrow{\gamma} \equiv \begin{pmatrix} \partial u_x/\partial x & \partial u_x/\partial y & \partial u_x/\partial z \\ \partial u_y/\partial x & \partial u_y/\partial y & \partial u_y/\partial z \\ \partial u_z/\partial x & \partial u_z/\partial y & \partial u_z/\partial z \end{pmatrix} = \frac{1}{a_0} \begin{pmatrix} \delta a_x & \delta b_x & \delta c_x \\ \delta a_y & \delta b_y & \delta c_y \\ \delta a_z & \delta b_z & \delta c_z \end{pmatrix} \tag{3}$$

where the u_i $(i = x, y, z)$ are the components of the displacement vector in the $(\boldsymbol{u}_x, \boldsymbol{u}_y, \boldsymbol{u}_z)$ basis. The components ε_{ij} $(i, j = x\ ,\ y\ ,\ z\ )$ of the strain tensor $\vec{\varepsilon}$ are then deduced from the well known relationship:

$$\varepsilon_{ij} = \frac{1}{2}\left[\frac{\partial u_i}{\partial x_j} + \frac{\partial u_j}{\partial x_i}\right]. \tag{4}$$

[a] e-mail: dufour@lpm.u-nancy.fr

Thus the averaged strain state in the probed region will be fully determined by the knowledge of the nine components of the lattice vectors deviations.

In a diffraction experiment however, one works in the reciprocal space in a basis defined in the usual way:

$$\boldsymbol{a}_0^* = 2\pi \frac{\boldsymbol{b}_0 \wedge \boldsymbol{c}_0}{\boldsymbol{a}_0 \cdot (\boldsymbol{b}_0 \wedge \boldsymbol{c}_0)}, \ldots \text{ and } \quad \boldsymbol{a}^* = 2\pi \frac{\boldsymbol{b} \wedge \boldsymbol{c}}{\boldsymbol{a} \cdot (\boldsymbol{b} \wedge \boldsymbol{c})}, \ldots \tag{5}$$

for both unstrained and strained samples, respectively. As in the real space, we define small reciprocal vectors deviations :

$$\begin{cases} \boldsymbol{\delta a}^* = \delta a_x^* \, \boldsymbol{u}_x + \delta a_y^* \, \boldsymbol{u}_y + \delta a_z^* \, \boldsymbol{u}_z \\ \boldsymbol{\delta b}^* = \delta b_x^* \, \boldsymbol{u}_x + \delta b_y^* \, \boldsymbol{u}_y + \delta b_z^* \, \boldsymbol{u}_z \\ \boldsymbol{\delta c}^* = \delta c_x^* \, \boldsymbol{u}_x + \delta c_y^* \, \boldsymbol{u}_y + \delta c_z^* \, \boldsymbol{u}_z \end{cases} \text{ with } \begin{cases} \boldsymbol{a}^* = \boldsymbol{a}_0^* + \boldsymbol{\delta a}^* \\ \boldsymbol{b}^* = \boldsymbol{b}_0^* + \boldsymbol{\delta b}^* \\ \boldsymbol{c}^* = \boldsymbol{c}_0^* + \boldsymbol{\delta c}^*. \end{cases} \tag{6}$$

The development of $\boldsymbol{a}^*$, $\boldsymbol{b}^*$ and $\boldsymbol{c}^*$ to the first order in the vectors deviations leads to linear relationships between the components of the vectors deviations in real and in reciprocal space which can be summarised in a matrix form:

$$\begin{pmatrix} \delta a_x^* & \delta b_x^* & \delta c_x^* \\ \delta a_y^* & \delta b_y^* & \delta c_y^* \\ \delta a_z^* & \delta b_z^* & \delta c_z^* \end{pmatrix} = -\frac{2\pi}{a_0^2} \begin{pmatrix} \delta a_x & \delta b_x & \delta c_x \\ \delta a_y & \delta b_y & \delta c_y \\ \delta a_z & \delta b_z & \delta c_z \end{pmatrix}^T \tag{7}$$

where the notation $(\ )^T$ stands for the transposed matrix.

In practice, one defines the reference cubic axes $(\boldsymbol{a}_0, \boldsymbol{b}_0, \boldsymbol{c}_0)$ attached to the sample through some conventions [4]. All reflections are lined up by adjusting the diffractometer angles (sample orientation and detector angle), and are indexed in this reference basis [4]: a Bragg reflection (hkl) ($\boldsymbol{Q} = \boldsymbol{G}_{hkl} = h\boldsymbol{a}^* + k\boldsymbol{b}^* + l\boldsymbol{c}^*$ with h, k and l integer numbers) is actually indexed as $(h_{exp} k_{exp} l_{exp})$ (with $\boldsymbol{Q} = h_{exp} \, \boldsymbol{a}_0^* + k_{exp} \, \boldsymbol{b}_0^* + l_{exp} \, \boldsymbol{c}_0^*$), where the h_{exp}, k_{exp} and l_{exp} experimental numbers deviate from h, k and l by small amounts $\delta h, \delta k$ and δl:

$$\begin{cases} h_{exp} = h + \delta h \\ k_{exp} = k + \delta k \\ l_{exp} = l + \delta l. \end{cases} \tag{8}$$

Identifying the two expressions for the diffraction vector $\mathbf{Q}$ and injecting (8) and (6) combined with (7), we obtain the relationships between the measured deviations $\delta h, \delta k$ and δl and the unknown components of the vectors deviations:

$$\begin{cases} h \, \delta a_x + k \, \delta a_y + l \delta \, a_z = -a_0 \, \delta h \\ h \, \delta b_x + k \, \delta b_y + l \delta \, b_z = -a_0 \, \delta k \\ h \, \delta c_x + k \, \delta c_y + l \delta \, c_z = -a_0 \, \delta l. \end{cases} \tag{9}$$

Thus, all these 9 components are experimentally determined from the indexation of at least 3 Bragg reflections. The strain tensor components are then obtained from (3) and (4). The method is further improved by measuring a higher number of reflections and refining the calculations through a least squares method [5], hence possibly eliminating systematic errors related to some misalignments [6].

Application: strain tensor determination in epitaxial Eu films

Following the preceding method, the strain tensor has been determined as a function of temperature in a 375 nm Eu(110) epitaxial thin film grown on a 50 nm Nb(110) buffer with the use of α-$Al_2O_3(11\bar{2}0)$ as a substrate. In order to avoid any contamination, the highly reactive Eu film was covered by a final 50 nm Nb layer. The epitaxial relationships between the Nb buffer and sapphire are well known [7], namely: $[\bar{1}11]_{\mathrm{Nb}} \parallel [0001]_{\mathrm{sapphire}}$ and $[\bar{1}1\bar{2}]_{\mathrm{Nb}} \parallel [\bar{1}100]_{\mathrm{sapphire}}$. Those between Nb(110) and Eu(110) are experimentally found to be : $[001]_{\mathrm{Eu}} \parallel [001]_{\mathrm{Nb}}$ and $[\bar{1}10]_{\mathrm{Eu}} \parallel [\bar{1}10]_{\mathrm{Nb}}$ [8].

The X-rays diffraction experiments were performed on the BM28 beamline at the ESRF, jointly with Resonant X-rays Magnetic Scattering (RXMS). The incident photons wavelength was tuned to 0.892 (1) Å. We must note here that the main purpose of the experiments was the characterization of the magnetic structure and its thermal behaviour, with the beamline actually optimised for magnetic scattering (polarisation and elimination of higher order contamination) rather than for strain determination (resolution). Although the experimental conditions were not optimum for strain determination, we will see below that the resolution was actually sufficient.

The sample was mounted in a closed cycle refrigerator on the 4-circle diffractometer. The automatic indexing of the reflections as a function of the diffractometer angles is included in the instrument software SPEC commonly used at the ESRF. In the chosen geometry, with the growth direction [110] and the $\boldsymbol{c}^*$ axis close to the scattering plane with all diffractometer angles set to zero, a convenient choice for the reference basis was $(\boldsymbol{a}_0^* + \boldsymbol{b}_0^*) \parallel (\boldsymbol{a}^* + \boldsymbol{b}^*)$ and $\boldsymbol{c}_0^*$ in the $(\boldsymbol{a}^* + \boldsymbol{b}^*, \boldsymbol{c}^*)$ plane. This was achieved by lining up the (440) and (350) Bragg peaks (the $\mathbf{h}_{1\varphi}$ and $\mathbf{h}_{2\varphi}$ vectors from reference [4], respectively).

The chosen reference lattice vectors $(\boldsymbol{a}_0, \boldsymbol{b}_0, \boldsymbol{c}_0)$ were that of "room" temperature ($T_0 = 269 \pm 4$ K) bcc bulk Eu, with lattice constant $a_0 = 4.58$ Å. For a better comparison with the behaviour of bulk Eu, strains in this paper will refer to this lattice constant at any temperature; so that the true strains for a given temperature (when writing elastic energy for example) will be obtained by subtracting the bulk Eu curve to the experimental data (see Figs. 1 and 2).

We measured the h_{exp}, k_{exp} and l_{exp} positions of five diffraction lines (namely: (440), (350), (352), (242) and (453)) at several temperatures in the range [285 K – 10 K]. At each temperature, the strain tensor was obtained by solving the set of $5 \times 3 = 15$ equations given by (9). The results are shown in Figure 1. For comparison, we also show the thermal behaviour of strains in bulk Eu (relatively to the 269 K lattice parameter) in the same reference basis, as derived from the experimental curve obtained by Bulatov and Kovalev on a Eu single crystal [9]. Comparison of absolute values between bulk Eu and the film is delicate due to both the poor calibration of the wavelength, and the uncertainty on the lattice constant of bulk Eu. However, considerations on variations are still reliable.

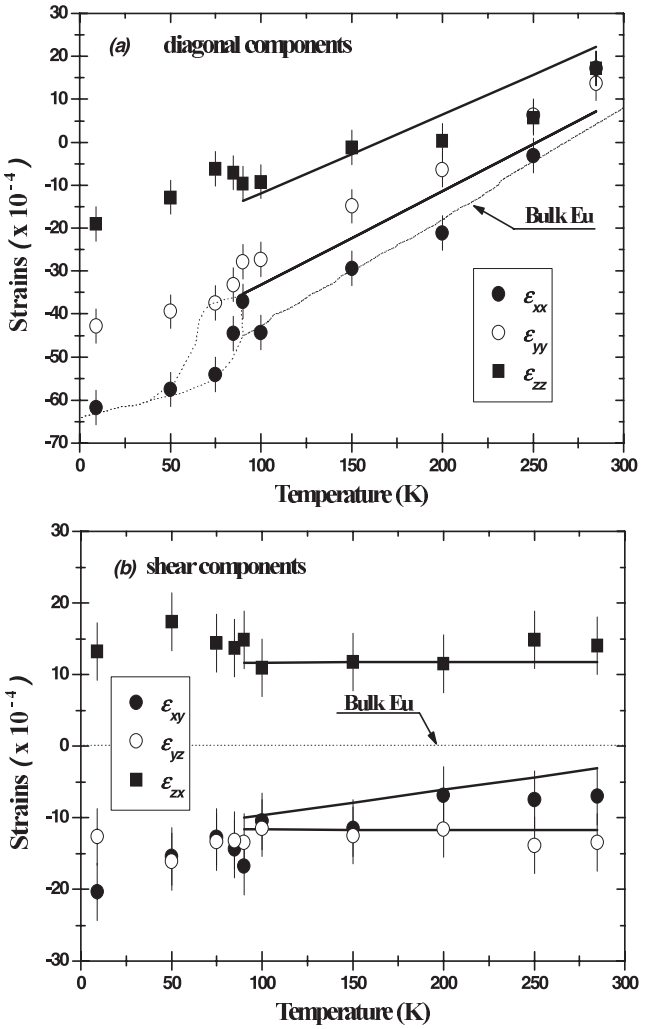

Fig. 1. Temperature dependence of the strains tensor components in the 375 nm Eu(110) film, in the $(\boldsymbol{u}_x, \boldsymbol{u}_y, \boldsymbol{u}_z)$ basis. The zero strains state refers to bulk Eu with $a_0 = 4.58$ Å. For comparison the bulk Eu behaviour is represented by the dashed lines obtained from reference [9]. The break at 90 K arises from the tetragonal distortion accompanying the helimagnetic transition. Bold lines are the tensor components obtained from the used biaxial strains model (see text).

We observe a linear evolution of the tensor components with decreasing temperature down to $T_N = 90$ K where RXMS shows that the Eu film undergoes a helimagnetic transition [3]. In bulk Eu this transition occurs at (89 ± 2)K (depending on the sample [9,10]) and is accompanied by a tetragonal distortion [9]. The breakdown of the linear behaviour of tensor components at 90 K is associated with this lattice distortion. This result constitutes the first experimental confirmation of the work of Bulatov and Kovalev [9]. Due to this distortion, the discussion in the following will mainly focus on the results obtained above T_N. Results below T_N will be briefly discussed at the end of this paper.

The diagonal components (Fig. 1a) bring information about the difference between strains in the film as compared to bulk Eu. The behaviour of ε_{zz} shows clearly that the contraction of the film along the [001] axis with decreasing temperature is smaller than in bulk Eu. The broken symmetry between the [100] and [010] axes has to be noted too: while the ε_{xx} component of the film approximately follows the bulk one, a distinct value is observed for ε_{yy}. The existence of non vanishing off-diagonal components (Fig. 1b), contrarily to bulk Eu, clearly indicates the presence of residual strains of thermal and/or epitaxial origin in the film. A deeper examination of these components shows that they seem to follow the relations $\varepsilon_{xy} \approx \varepsilon_{zy} \approx -\varepsilon_{xz}$ over the whole temperature range, although absolute values are within the uncertainty on the wavelength.

Actually, for a better understanding of the strains state inside the film, a different reference basis, linked to the particular directions of the film seems more convenient. The first direction is the [110] growth direction while the other two lie in the growth plane: either $[\bar{1}10]$ and [001] because of the epitaxial relationships between Nb(110) and Eu(110), or $[\bar{1}11]$ and $[1\bar{1}2]$ because of the epitaxial relationships between Nb(110) and α-$Al_2O_3(11\bar{2}0)$, which may influence the observed strains in the Eu(110) film. The full data analysis with either basis showed that the second one leads to a simpler description of the strains. We will call ε'_{ij} the strain tensor components expressed in this new basis, $\{\boldsymbol{u'}\} = \left(\boldsymbol{u}_{[110]}, \boldsymbol{u}_{[\bar{1}11]}, \boldsymbol{u}_{[1\bar{1}2]}\right)$.

Figure 2 shows the experimental tensor components ε'_{ij} in the $\{\boldsymbol{u'}\}$ basis. The first important information is given by the ε'_{11} component (full circles in Fig. 2a) which follows the bulk value over the whole temperature range. This shows that the observed strain along the growth direction is only due to the bulk Eu thermal effect with no influence from the substrate. On the contrary, we observe a slight change of slope in the temperature dependence of the in-plane diagonal components ε'_{22} and ε'_{33} (open circles and full squares in Fig. 2a, respectively). More striking in Figure 2a is the huge difference between the ε'_{33} values of the film and that of the bulk. Finally, the off-diagonal tensor components fall within the experimental error at all temperatures (Fig. 2b): in first approximation, no shear strains are observable in this basis and we can write the experimental strains state inside our Eu film in the form:

$$\overleftrightarrow{\varepsilon}'(T) \approx \begin{pmatrix} \varepsilon'_{11}(T) & 0 & 0 \\ 0 & \varepsilon'_{22}(T) & 0 \\ 0 & 0 & \varepsilon'_{33}(T) \end{pmatrix}$$

where $\varepsilon'_{11}(T)$ is equal to the bulk Eu curve calculated from reference [9], $\varepsilon'_{11}(T) = \varepsilon'^{\mathrm{Eu}}_{11}(T) = \alpha_{\mathrm{Eu}}\,(T - T_0)$, where α_{Eu} is the thermal expansion coefficient of bulk Eu, $\alpha_{\mathrm{Eu}} = 25 \times 10^{-6}$ K^{-1} [11], and T_0 is the temperature for which the lattice parameter of Eu is $a_0 = 4.58$ Å (i.e. the zero strains state in this work). Within this approximation, the contribution of the substrate to the strain field can be viewed as biaxial, a model commonly used for a cubic symmetry. $\varepsilon'_{22}(T)$ and $\varepsilon'_{33}(T)$ are obtained from a linear fit of the experimental data: these in-plane components are modelled in terms of thermal strains originating from unequal thermal expansion coefficients between the

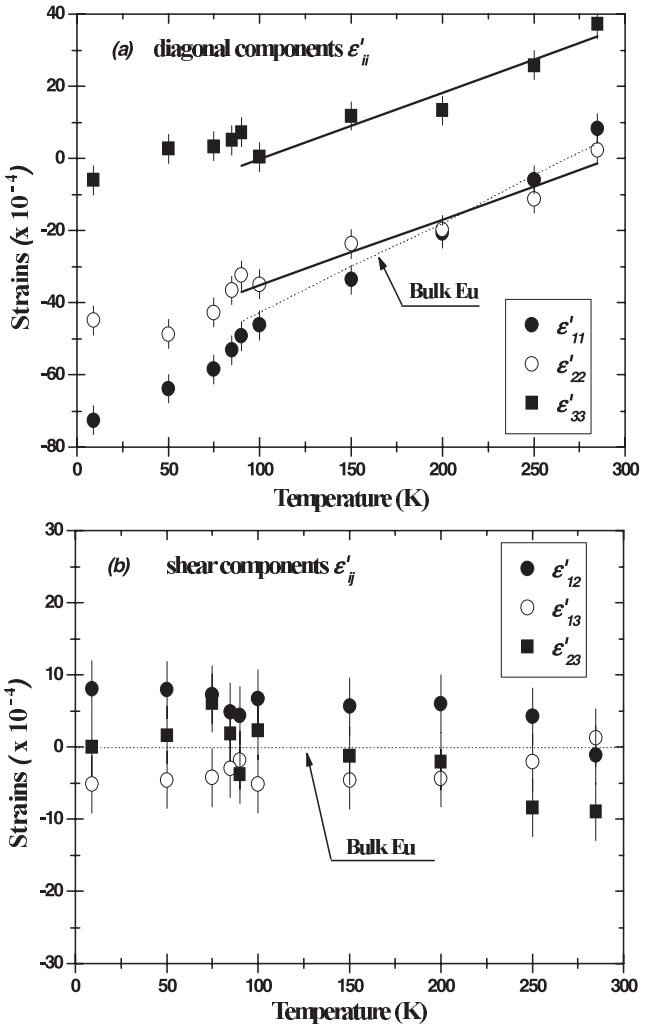

Fig. 2. Temperature dependence of the strains tensor components in the $(\boldsymbol{u}_{[110]}, \boldsymbol{u}_{[\bar{1}11]}, \boldsymbol{u}_{[1\bar{1}2]})$. Bold lines are linear fits to the data used for the biaxial strains model (see Tab. 1).

Table 1. Results of linear fits of the $\varepsilon'_{ii}(T)$ curves in the temperature range [90 K–285 K].

$a+bT$ fit	$a(\times 10^{-4})$	$b(\times 10^{-6}$ K$^{-1})$
Bulk Eu [8]: $\varepsilon'^{\mathrm{Eu}}_{11}(T)$	-68.2 ± 0.5	25.3 ± 0.2 (α_{Eu})
$\varepsilon'_{11}(T)$	-73 ± 2	26 ± 2
$\varepsilon'_{22}(T)$	-53 ± 5	18 ± 2
$\varepsilon'_{33}(T)$	-19 ± 6	18 ± 2

film and the substrate:

$$\varepsilon'(T) = \varepsilon'(T_0) + (\alpha_f - \alpha_s)\,(T - T_0) = a + bT$$

where $\varepsilon'(T_0)$ is the residual strain, of thermal and/or epitaxial origin, at the reference temperature T_0; α_f and α_s are the thermal expansion coefficients of the film and the substrate respectively. The results of the linear fits are summarised in Table 1.

The substrate is made from the Nb buffer epitaxially grown on α-sapphire, two materials with similar expansion coefficients, around $(5 \pm 2) \times 10^{-6}$ K^{-1} for α-sapphire [12,13] at 300 K (the variations depend on the directions involved), and around 7×10^{-6} K^{-1} for Nb [14]. The thermal expansion of the Nb buffer is likely influenced by α-sapphire, but we must here consider the substrate as a whole (Nb + α-sapphire). We find $\alpha_s = \alpha_{\mathrm{Eu}} - b = (7 \pm 2) \times 10^{-6}$ K^{-1}, consistent with the above values.

An estimation of $\varepsilon'(T_0)$ for the two in-plane tensor components is obtained from the a values of Table 1: $\varepsilon'_{22}(T_0) = (-5 \pm 5) \times 10^{-4}$ and $\varepsilon'_{33}(T_0) = (29 \pm 6) \times 10^{-4}$. As already pointed out, $\varepsilon'(T_0)$ is the sum of residual thermal strain and epitaxial strain at T_0 which can hardly be separated. However, these results indicate that most of the residual strain in our Eu film is along the $[1\bar{1}2]$ direction (i.e. $\varepsilon'_{33}(T)$). This may be correlated with the existence of strains along this direction in epitaxial Nb(110) on the $(11\bar{2}0)$ sapphire [15] which induce the formation of misfit dislocations.

To complete the physical interpretation of these ε'_{ii} and estimate the limits of our approximated strain state, we now come back to the original $(\boldsymbol{u}_x, \boldsymbol{u}_y, \boldsymbol{u}_z)$ basis and derive the $\varepsilon_{ij}(i, j = x, y, z)$ tensor components from the fitted $\overleftrightarrow{\varepsilon}'(T)$ tensor. The results are represented by bold lines in Figure 1. Clearly, all the off diagonal components are fairly well reproduced. Actually, these components have non zero values because $\varepsilon'_{33}(T)$ and to a lesser extent $\varepsilon'_{22}(T)$, differ from the bulk Eu curve. The $\varepsilon_{zz}(T)$ curve is reproduced too, although the slope of the line is slightly overestimated. But it is especially in the estimation of ε_{xx} and ε_{yy} that a net breakdown occurs. It is not surprising at all, because within this approximation ε_{xx} and ε_{yy} have to be symmetric due to the assumed nullity of the ε'_{12} and/or ε'_{13} components. Thus, it would be necessary to give a finite value to these components in order to reproduce the experimental behaviour of ε_{xx} and ε_{yy}, meaning that the true strains state inside the film is not totally confined in the plane of growth. At the same time, one should also give a finite value to ε'_{23}, which is of same magnitude as ε'_{12} and/or ε'_{13}, with the consequence to improve the estimation of $\varepsilon_{zz}(T)$. To summarise, the $\overleftrightarrow{\varepsilon}'(T)$ tensor given above is a good approximation of the experimental strains state in the film, except for the diagonal components ε_{xx} and ε_{yy}.

Finally, a brief comment about our results below T_N is necessary. In bulk Eu, the helimagnetic order is associated with a helical propagation vector along the $\langle 100 \rangle$ axis of the cube, the magnetic moments lying in the perpendicular planes [10]. The tetragonal distortion coming with the magnetic transition consists of an elongation along the direction of the propagation vector and a contraction in the perpendicular plane. The consequence is to separate the single crystal into three crystallo-magnetic domains. In our Eu film, RXMS experiments show that it is the case except for a slight shift in the orientation of the propagation vectors with the $\langle 100 \rangle$ bulk axis [3]. Nevertheless, the tensor components we found in this range of temperatures have to be considered as averaged values over the three crystallo-magnetic domains.

Conclusion

A simple method has been proposed for the determination of strains in a single crystal by using X-ray diffraction experiments and the accurate determination of the positions of several Bragg peaks in reciprocal space. In principle, three diffraction lines have to be measured in order to completely specify the strain tensor. However, in practice, due to the experimental errors, the measurement of more lines is needed. This method has been applied on a Eu epitaxial thin film showing that, in a first approximation, the thermal and epitaxial strains are essentially located along the $[1\bar{1}2]$ direction in the plane of growth.

References

1. A. Mougin, C. Dufour, K. Dumesnil, Ph. Mangin, Phys. Rev. B **62**, 1136 (2000); K. Dumesnil, C. Dufour, Ph. Mangin, G. Marchal, M. Hennion, Europhys. Lett. **31**, 43 (1995)
2. B.M. Clemens, J.A. Bain, MRS Bull. July 1992, pp. 46-51; I.C. Noyan, J.B. Cohen, *Residual Stress Measurements by Diffraction and Interpretation* (New-York, Springer Verlag, 1987)
3. S. Soriano, K. Dumesnil, C. Dufour, T. Gourieux, Ph. Mangin, A. Stunault, Phys. Rev. B **71**, 092409 (2005)
4. W.R. Busing, H.A. Levy, Acta Cryst. **22**, 457 (1967)
5. W.H. Press, S.A. Teukolsky, W.T. Vetterling, B.P. Flannery, *Numerical Recipes in Fortran*, 2nd edn. (Cambridge University Press, 1992), p. 665
6. J. Jo, R.W. Hendricks, J. Appl. Cryst. **24**, 878 (1991)
7. For a recent review, see: A.R. Wildes, J. Mayer, K. Theis-Bröhl, Thin Solid Films **401**, 7 (2001)
8. S. Soriano, K. Dumesnil, C. Dufour, D. Pierre, J. Cryst. Growth **265**, 582 (2004)
9. A.S. Bulatov, O.V. Kovalev, Sov. Phys. Solid State **30**, 266 (1988)
10. N.G. Nereson, C.E. Olsen, G.P. Arnold, Phys. Rev. **135**, A176 (1964)
11. This value of α_{Eu} is derived from the data of Bulatov and Kovalev [9] who worked on a single crystal below 300 K. The value $\alpha_{Eu} = (24 \pm 4) \times 10^{-6}$ K^{-1} was found by A.M. Burkhanov, N.P. Grazhdankina, I.G. Fakidov, Sov. Phys. Sol. State **9**, 586 (1967), by using a differential tensometry method on a polycristalline sample below 300 K. Other values lying around 33×10^{-6} K^{-1} in polycrystalline Eu have been obtained above room temperature: see Beaudry et al., J. Less Com. Met. **34**, 225 (1974) and Spedding, Hanak and Daane, J. Less. Com. Met. 1960
12. J.B. Wachtman, T.G. Scuderi, G.W. Cleek, J. Am. Ceram. Soc. **45**, 319 (1962)
13. M. Leszczynski, T. Suski, H. Teisseyre, P. Perlin, I. Grzegory, J. Jun, S. Porowski, T.D. Moustakas, J. Appl. Phys. **76**, 4909 (1994)
14. *Handbook of Chemistry and Physics*, edited by D.R. Lide (CRC Press, 1994), pp. 12–160
15. E.J. Grier, M.L. Jenkins, A.K. Petford-Long, R.C.C. Ward, M.R. Wells, Thin Solid Films **358**, 94 (2000)